Research Article

Sibilla Di Pace*, Arwa Dabbech, Vitalii Khodnevych, Michel Lintz, and Nicoleta Dinu-Jaeger

Particle contamination monitoring in the backscattering light experiment for LISA

https://doi.org/10.1515/oms-2019-0002
Received Dec 10, 2018; accepted Mar 25, 2019

Abstract: In the context of space-based optics, contamination due to particle deposition on the optics is inevitable and constitutes a critical issue. This gets more challenging for the sensitive heterodyne measurements of the Laser Interferometer Space Antenna (LISA), the space-based gravitational wave observatory to be launched in 2034. Therefore, table-top experiments need to be developed for a better understanding of how micrometer to millimeter sized dust particles, present on optical surfaces, affect LISA measurements. In this work, we present an experimental setup for the simultaneous measurement of the coherent backscattering and the monitoring of particles deposition on the optics to be tested. The results of the first measurements are presented and discussed in this article.

Keywords: Straylight, backscattering, heterodyne, space, interferometer

1 LISA and the back-scattered light issue

The Laser Interferometer Space Antenna (LISA) is a L-class ESA mission, starting the phase A. It will be a space-based gravitational wave (GW) observatory composed of a constellation of three spacecrafts (S/C) in equilateral configuration, orbiting at 1A.U. around the Sun [1, 2]. Each spacecraft will host and constantly follow two free-falling test masses (TMs) only subjected to the gravitational force. The presence of seismic noise prevents the observation of GW sources below 1Hz on Earth [3]. This issue can be overcome by going to space. LISA sensitivity curve will cover the frequency range from 0.1mHz to 1Hz, that is a window of observation complementary to those of ground based GW interferometers. Therefore, LISA will be able to observe other important sources, such as GWs from cosmological stochastic background, and sources detectable from Earth years or months before they enter in the frequency range of the ground based GW detectors [1, 2]. Moreover, thanks to its orbital configuration, LISA will be able to detect GW sources coming from all directions in the sky.
The LISA mission has two main conceptual basic functions and technological challenges [1, 2]:

- drag-free system: μ-thrusters to adjust the S/C position to keep the test masses (TMs) in free-falling condition;
- interferometric measurement to monitor arm-length changes within a noise of $\sim 10pm/\sqrt{Hz}$ in the range 0.1 mHz-1 Hz.

The former has been successfully tested by the technology demonstrator of LISA, the LISA Pathfinder (LPF), while the interferometric measurement requirements of LISA [2] could not be tested with the single satellite of LPF. In LISA, S/Cs will be identical and each one will host two laser links, two optical benches and two telescopes. Each telescope will transmit the beam towards the distant S/C and will receive back the signal from the distant S/C. The transmitted power will be $T_x \sim 2W$ while the received power will be $R_x \sim 700pW$ only. Therefore, if the transmitted power is partially backscattered (due to optics imperfections: roughness, dusts, etc.) into the optical bench and reaches the detection photodiodes, this may seriously affect the sensitive heterodyne measurements of LISA. The interferometric measurement to monitor arm-length changes should have a noise lower than $10pm/\sqrt{Hz}$ [2], which implies a noise allocation of less than $1\,\mu cycle/\sqrt{Hz}$. This issue sets an important requirement: even stray beams with a relative power as low as a few 10^{-12} can significantly degrade the noise in the arm-length measurement. This critical issue should be investigated in detail at the present time as well as in the next years. Therefore, table-top ex-

***Corresponding Author: Sibilla Di Pace:** Laboratoire ARTEMIS, Université Côte d'Azur, Observatoire de la Côte d'Azur and CNRS, Nice, France; now at Università degli Studi di Roma La Sapienza e INFN Sezione di Roma, Rome, Italy; Email: sibilla.dipace@roma1.infn.it
Arwa Dabbech: Institute of Sensors, Signals and Systems, Heriot-Watt University, Edinburgh, United Kingdom
Vitalii Khodnevych, Michel Lintz, Nicoleta Dinu-Jaeger: Laboratoire ARTEMIS, Université Côte d'Azur, Observatoire de la Côte d'Azur and CNRS, Nice, France

periments like the one presented in this paper, need to be developed for a better understanding of how micrometer to millimeter sized dust particles, on optical surfaces, affect LISA measurements.

2 Experimental set-up

We have designed and realised an experiment for the remote constant monitoring of dust deposition on a mirror surface via a reflex camera and developed an image processing method to analyse the pictures. The set-up, as shown in figure 1, consists of a 12.5mm diameter mirror under test (MUT) placed on a micrometric translation stage for the fine adjustment of the focus and shined from the side by a led light and a focusing lens. We use a remotely controlled reflex camera with a macro objective [1] constantly looking at the MUT and taking pictures. This set-up is integrated with a homodyne Michelson interferometer designed to measure the coherent backscattering (CBS) from an optical surface with small roughness or contamination. Once integrated, the two experiments allow us to correlate the CBS signal with the physical properties of the dust particles identified on the MUT.

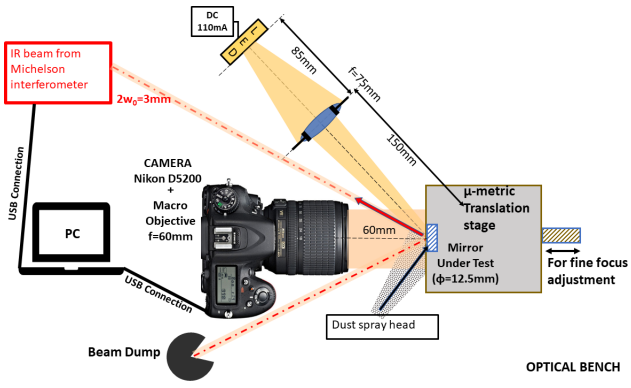

Figure 1: Simplified scheme of the experimental set-up. A reflex camera with a macro objective constantly looks at the mirror under test (MUT) placed on a micrometric translation stage and shined from the side by a led and a focusing lens. The mirror is also sensed by a Michelson interferometer with IR laser. In this part of the set-up there is the piezo modulation of the optical path. The connection with the PC allows to remotely control the camera and to record the inteferometric signal. A dust spray system allows artificial deposition of particles on the mirror.

3 Measurements

We have realised a table-top experiment, as depicted in figure 1, with the aim of understanding the effects of backscattering in the interferometric measurements of LISA. This set-up works in conditions similar to those of LISA measurements, although much simplified. This will help us to model out from the measurements and the analysis methods. Our table-top experiment is composed of two main parts: the partially fibered Michelson interferometer, and the dust deposition monitoring set-up. The first part is used to measure the coherent backscattering signal and operates with an infrared laser diode source of wavelength 1.542μm. One arm of the Michelson is totally fibered and the other arm has only the last end of its optical path in the air, in order to place the optics to be tested on the optical bench. The optical path in the air of the Michelson interferometer is constituted of a collimator, a highly reflecting mirror installed on a piezoelectric actuator to modulate the optical path of the beam at a frequency of 2kHz (inside the red box represented in figure 1), the mirror under test (MUT) and a beam dump. The optical bench which hosts all these optics is installed inside a clean tent under a laminar flux to keep the critical optics clean. The mirror under test constitutes the link between the Michelson set-up and the dust monitoring set-up. In order to realise the dust deposition without contaminating the other optics, this part of the set-up needs to be placed in a less clean area. Therefore, we have installed a second smaller optical bench next to the Michelson's one, but outside the clean tent, for integrating the two parts of the experimental set-up (as in the scheme of figure 1). The artificial dust deposition is realised with a spray system composed of a motor, a small reservoir, where we put monodispersed silica spheres diluted in ultraclean propanol, and a sharp head (see figure 2). This system allows us to realise sprays of controlled duration and concentration of known size silica spheres. For the measurements, we use silica spheres having diameter $d = (16.04 \pm 0.35)$ μm. For the realisation of the parallel measurements of coherent backscattering and dust deposition monitoring, we register the interferometric signal and simultaneously take a picture of the mirror before and after each dust-spray of particles on the mirror. A calibration picture to recover the center of the laser beam is obtained using a visible red laser sent towards the mirror under test along the optical path in the air of the Michelson set-up.

1 https://www.nikon.co.uk/en_GB/product/nikkor-lenses/auto-focus-lenses/fx/single-focal-length/af-s-micro-nikkor-60mm-f-2-8g-ed

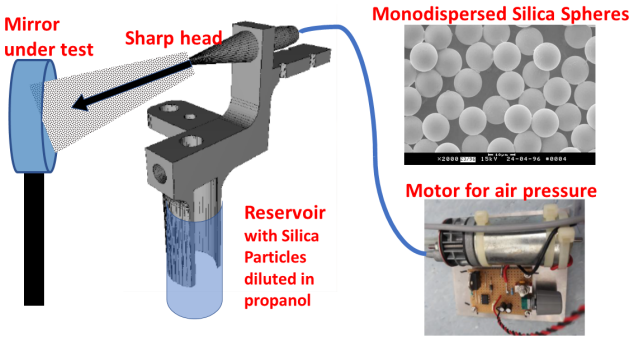

Figure 2: Detailed representation of the artificial dust deposition system or dust spray system. The small reservoir contains monodispersed silica spheres (detailed view on the top right) diluted in ultra clean propanol. A motor for air pressure (bottom right) allows to spray the solution of propanol and silica spheres on the mirror with controlled duration. We used silica spheres of diameter $d = (16.04 \pm 0.35)$ µm.

4 Image processing and analysis

Dust particles are analysed via image processing techniques implemented in MATLAB. The pictures of the mirror under test, with dusts deposited on its surface, resemble a dark sky full of stars, or other bright sources. Therefore, for the image processing, we have optimised an image reconstruction method originally developed for astronomical images [4]. The analysis on the parallel measurements of coherent backscattering and dust deposition monitoring can be done on a restricted surface of the mirror: the one sensed by the IR laser beam spot on the MUT. Images taken by the camera are of size 6000x4000 pixels, covering the whole mirror under test and a wide dark area around. For the purpose of our study, we restrict the analysis to the area sensed by the laser which is the only part influencing the coherent backscattering signal detected by the Michelson interferometer. In the present case, the IR beam has a spotsize radius on the MUT of 1.7 mm. In figure 3 we report an example of image reconstruction of the area delimited by a circle of radius 1.7 mm.

4.1 Image processing

Our imaging methodology is described in the following. In the first instance, a sparse and positive image composed of compact structures is estimated from the original image using convex optimisation theory and sparse representations framework [4]. The approach involves two hyperparameters representing the tradeoff between sparsity of the reconstructed and its goodness-of-fit to the original image. The reconstructed image is then analysed via MATLAB built-in functions where segmentation is performed, followed by the classification of the detected spots (size, position, flux, peak intensity). Following the image reconstruction, a Gaussian fit is performed on each of the identified bright sources to extract information on their major and minor axis, spot area, flux and peak intensity. Figure 3 shows an example of one original image (on the left), the reconstructed image consisting of the estimated sources (at the center) and the image consisting of Gaussians, where the Gaussian fit has been applied on the detected sources (on the right). The smallest spot-source identified with the image processing has a diameter of 5 µm, while the camera sensor pixel-size is 3.9 µm. Identified spot-sizes range from 5 µm to 390 µm. In our pictures the pixel-size, and thus the pixels separation, corresponds to 5 µm. This value is slightly better than the 7-8 µm that can be expected from the MTF (modulation transfer function) of the macro objective lens presented in the manufacturer's documentation.

4.2 Analysis

Tables 1 and 2 summarise the values retrieved from the image processing and the analysis of the interferometric signal to reconstruct the coherent backscattering relative amplitude, for the two data sets collected. N_{tot} is the total number of sources detected with the image processing restricted to the circular area covered by the laser spot. How-

Table 1: Table reporting the data set taken on the 20/9/2018. N_{tot} is the total number of sources retrieved with the image processing code, N_e is the sub-set of N_{tot} having eccentricity $0 \leq e \leq 0.29$, and N_d is the sub-set of N_e having diameter $10\mu m \leq d \leq 22\mu m$. CBS is the measured value of relative backscattering amplitude (see equation 1).

RUN	N_{tot}	N_e	N_d	CBS ($\times 10^{-6}$)
0	253	96	19	2.335 ± 0.817
1	281	88	16	1.719 ± 0.747
2	1591	458	68	1.311 ± 0.684
3	1054	336	57	2.713 ± 0.936
4	1798	414	62	1.48 ± 1.03
5	2061	436	69	2.375 ± 0.984
6	925	305	48	2.919 ± 0.802
7	1162	286	53	1.676 ± 0.801
8	700	193	37	3.266 ± 0.784
9	486	153	28	1.003 ± 0.497
10	1083	258	46	1.753 ± 0.932
11	573	179	27	3.03 ± 1.05
12	734	215	38	2.129 ± 0.914

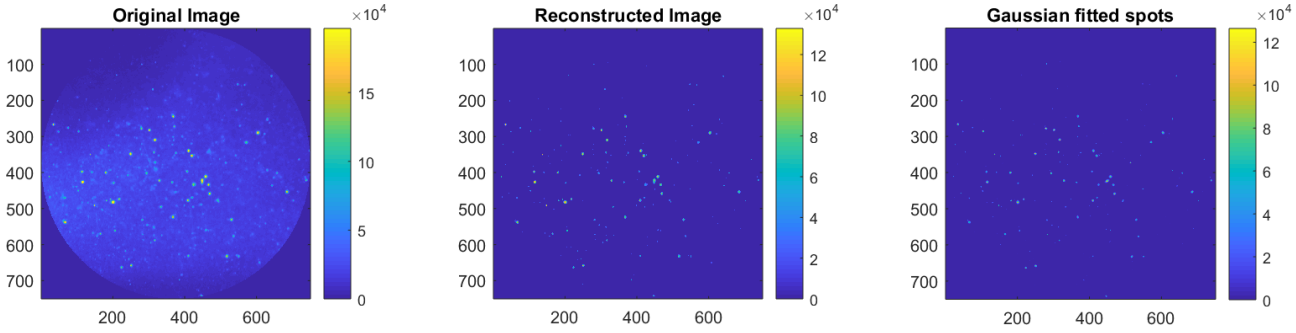

Figure 3: Example of the reconstruction with the image processing technique restricted on the area seen by the laser. The original image is on the left, the reconstructed one in the center and the one where Gaussian fit has been applied on the detected sources on the right. The units of the x-y axis are in pixels. The colour bar corresponds to the pixels values as exported from the image file as a matrix and expressed in arbitrary units.

Table 2: Table reporting the data set taken on the 4/10/2018. N_{tot} is the total number of sources retrieved with the image processing code, N_e is the sub-set of N_{tot} having eccentricity $0 \leq e \leq 0.29$, and N_d is the sub-set of N_e having diameter $10\mu m \leq d \leq 22\mu m$. CBS is the measured value of relative backscattering amplitude (see equation 1).

RUN	N_{tot}	N_e	N_d	CBS ($\times 10^{-6}$)
0	424	99	12	1.63 ± 1.10
1	402	105	17	1.900 ± 0.953
2	305	74	11	1.74 ± 1.07
3	304	59	8	1.620 ± 0.790
4	162	37	7	1.71 ± 1.02
5	352	84	19	1.620 ± 0.771
6	256	46	6	1.820 ± 0.607
7	288	59	12	1.750 ± 0.703
8	205	38	6	1.830 ± 0.763
9	277	77	8	1.700 ± 0.617
10	382	78	11	1.860 ± 0.634

ever, the particles we want to retrieve with the image processing are the monodispersed silica spheres having a diameter $d = (16.04 \pm 0.35)$ µm. Therefore, we want to restrict the selection of the retrieved particles on the basis of the information on the diameter dimension and on the fact that they are not perfectly spherical. As a first step, we considered the error on the diameter by selecting particles with eccentricity comprised between zero and 0.29 which corresponds to an ellipse having major axis (16.04 + 0.35) µm = 16.39 µm and minor axis (16.04 – 0.35) µm = 15.69 µm. This selection led us to a sub-set of N_{tot}, the number of particles N_e having eccentricity $0 \leq e \leq 0.29$. For a more stringent choice of the artificially deposited particles to retrieve, in addition to the selection on the eccentricity, we choose the sub-set of N_e particles having diameter values close to 16 µm with an error corresponding to

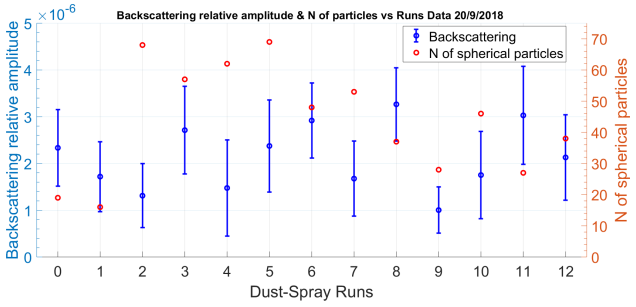

Figure 4: Plot of the coherent backscattering relative amplitude and of the number of spherical particles N_d retrieved from the pictures as a function of the dust spray runs for the data set taken on the 20/9/2018.

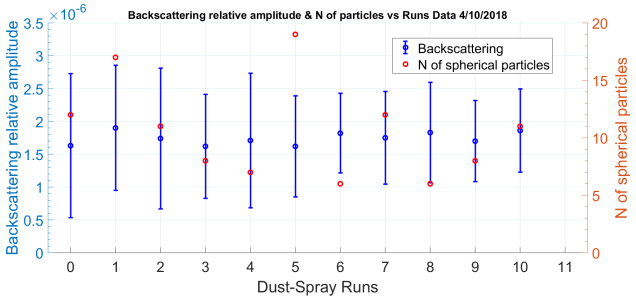

Figure 5: Plot of the coherent backscattering relative amplitude and of the number of spherical particles N_d retrieved from the pictures as a function of the dust spray runs for the data set taken on the 4/10/2018.

about one pixel. This choice results in a number of particles N_d, which is a sub-set of N_e having diameters 10 µm ≤ d ≤ 22 µmm. We then plot the number of the retrieved particles N_d and the coherent backscattering amplitude measured, as a function of the run of dust-sprays for each data set collected (figures 4 and 5). The backscattering relative

amplitude is calculated with the following formula:

$$\sqrt{b_S} = \frac{1}{I_L/2}\sqrt{\left(\frac{R_1}{2J_1(2\pi\delta)}\right)^2 + \left(\frac{R_2}{2J_2(2\pi\delta)}\right)^2} \quad (1)$$

where $R_{1,2}$ are the first and second harmonic of the beam path modulation with the piezo mirror at 2kHz, $J_{1,2}$ are the Bessel's functions of the first kind (first and second order respectively), $I_L/2$ is the calibration coefficient measured when the mirror under test is replaced by a metal mirror at normal incidence, and δ is the modulation depth of the piezo mirror (PM). The formula of equation 1 has been calculated from the output signal of the interferometer. After a full round trip along the two arms of the Michelson interferometer, the signal gains a phase $\Delta\phi_S$ which corresponds to the optical path difference of the two arms, where one is fully fibered and the other partially fibered. Thus, the interferometric signal at the detection photodiode is:

$$I = \frac{I_L}{2}\sqrt{b_S}\cos\Delta\phi_S \quad (2)$$

where b_S is the backscattering relative amplitude that we want to measure. In order to extract the signal amplitude, we introduce a piezo actuator on one mirror in free space (the so called piezo-mirror (PM)) for the modulation of the optical beam path. This modulation on the PM has amplitude δ and frequency ω. The interferometric signal thus becomes:

$$I = \frac{I_L}{2}\sqrt{b_S}\cos(\phi + \delta\sin(\omega t)), \quad (3)$$

where ϕ is an arbitrary phase offset. According to the expansion in series of Bessel functions [7], the $\cos(\phi + \delta\sin(\omega t))$ can be rewritten as follows:

$$J_0(\delta)\cos\phi + 2\Sigma_n J_{2n}(\delta)\cos(2n\omega t)\cos\phi \quad (4)$$
$$- 2\Sigma_n J_{2n-1}(\delta)\cos((2n-1)\omega t)\sin\phi.$$

The fringe signal (equation 3) is demodulated at the frequency $\omega/2\pi$ (we thus record the amplitude $R_1(t)$ of the modulated signal) and at the frequency $2\cdot\omega/2\pi$ (we record the amplitude $R_2(t)$). Since our set-up is not temperature-stabilised, the phase offset ϕ drifts slowly, and so both

$$R_1(t) = I_L\sqrt{b_S}J_1(2\pi\delta)\cos(\phi(t)), \quad (5)$$
$$R_2(t) = I_L\sqrt{b_S}J_2(2\pi\delta)\sin(\phi(t)),$$

where $J_{1,2}$ are the Bessel's functions of the first kind. Since $\cos^2\phi(t) + \sin^2\phi(t) = 1$, the expression of equation 1 allows to eliminate this fluctuation and to retrieve the backscattering amplitude $\sqrt{b_s}$.

5 Comparison with theory

The conditions of our measurements of coherent backscattering from silica spheres deposited on a plane mirror can be described within Mie theory. We first recall that our conditions satisfy Mie's hypothesis for the diffraction of a plane monochromatic wave by a homogeneous sphere of any diameter and any composition situated in a homogeneous medium [5]. Another important assumption to consider is that the beam transverse extent (beam radius) should be infinite with respect to the sphere radius, or at least 10 times bigger [6]. Our set-up satisfies this condition since the beam radius is $1.7mm$, while the sphere radius is 8 µm. The present model also applies to diffraction by any number of spheres, provided that they are all of the same diameter and composition and also that they are randomly distributed and separated from each other by distances that are large compared to the wavelength. The total scattered power is then equal to the power scattered by one sphere multiplied by their total number [6]. In our case, 50 µm is the average distance between identical sphere particles, evaluated after image processing, while we recall that the wavelength is 1.542 µm. Therefore, we can affirm that our experiment satisfies the conditions previously enunciated according to Mie theory. The summation for estimating the scattering field is infinite, but it has been empirically demonstrated [6] that a very good approximation consists in stopping the summation at a value N_c which is the closest integer to: $N_c = x + 4x^{1/3} + 2$, where x is the size parameter defined as:

$$x = \kappa a = \frac{2\pi n}{\lambda}a \quad (6)$$

in which n is refractive index of the medium, λ the wavelength, and $a = d/2$ the sphere radius. Moreover, if we are in the regime $\kappa r \gg N_c^2$ (with r the distance of the scattered field from the scattering sphere) the components of the scattered field can be written in the simple form [6]:

$$E_{s,\theta} = E_0\frac{e^{i\kappa r}}{-i\kappa r}\cos\phi\cdot S_2(\cos\theta), \quad (7)$$

$$E_{s,\phi} = -E_0\frac{e^{i\kappa r}}{-i\kappa r}\sin\phi\cdot S_1(\cos\theta), \quad (8)$$

where $S_{1,2}$ are the Mie scattering functions, θ, ϕ are the scattering angle and the azimuthal angle of the scattering plane with respect to the incident direction. In our case $N_c = 47$, $r = 25cm$, so that the conditions mentioned above are satisfied ($1.02\cdot 10^6 \gg 2209$) and the scattered intensity can be written as follows:

$$I_s(\theta) = |E_{s,\theta}|^2 + |E_{s,\phi}|^2 \quad (9)$$

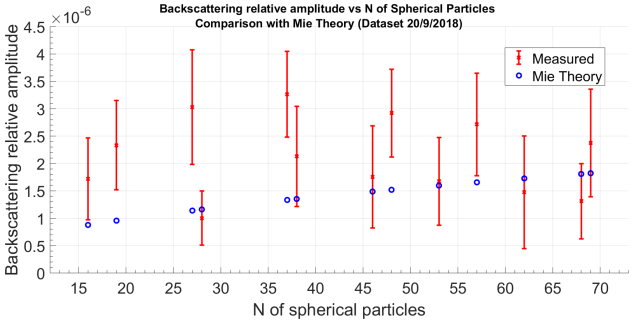

Figure 6: Comparison of the relative backscattering amplitude measured and estimated from Mie theory as a function of the number of spherical silica particles N_d retrieved from image processing for each dust-spray run for the data set of the 20/9/2018.

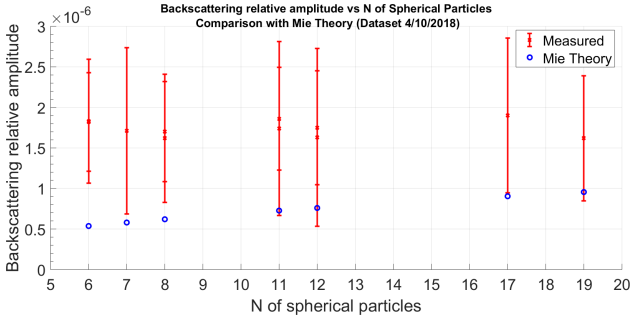

Figure 7: Comparison of the relative backscattering amplitude measured and estimated from Mie theory as a function of the number of spherical silica particles N_d retrieved from image processing for each dust-spray run for the data set of the 4/10/2018.

$$= \frac{E_0^2}{(\kappa r)^2}\left[|S_2(\cos\theta)|^2(\cos\phi)^2 + |S_1(\cos\theta)|^2(\sin\phi)^2\right].$$

Furthermore, since we are considering the backscattered intensity, $\phi = \pi/4$ and $\theta = \pi$, so equation 9 becomes:

$$I_s(\theta = \pi) = \frac{E_0^2}{2(\kappa r)^2}\left[|S_1|^2 + |S_2|^2\right]. \tag{10}$$

For comparison with the measured data, we multiply the intensity of equation 10 by the solid angle Ω seen by the detector, and by the number of spherical particles. In our experimental set-up, the backscattered intensity enters in the interferometer through the fiber collimator, which thus gives us the value of the solid angle seen by the detector $\Omega = \mathcal{A}/r^2 = \pi(BD/2)^2/r^2$,
where BD is the beam diameter defined as $BD = 2fN.A.$, with f the focal length of the collimator lens, $N.A.$ the numerical aperture of the fiber. Therefore, the relative backscattering amplitude estimated from Mie theory can be written as:

$$\sqrt{b_{S,Mie}} = \sqrt{\frac{1}{2(\kappa r)^2}\left[|S_1|^2 + |S_2|^2\right] \cdot \Omega \cdot N_{part}} \tag{11}$$

where N_{part} is the number of spherical particles retrieved from the image processing analysis. Following the assumptions stated at the beginning of this section, Mie theory allows us to model the backscattering effect of identical spherical particles. In order to compare theory and measurements, we have focused the analysis on the spherical particles artificially deposited on the mirror under test. The figures 6 and 7 showcase the backscattering relative amplitude measured with the formula of equation 1 as a function of the number of retrieved spherical particles (N_d), for each data set, also compared with the values expected according to Mie theory (equation 11).

6 Conclusions

The parallel measurements of the interferometric signal and of the pictures of the mirror under test, allowed us to compare the coherent backscattering signal with the apparition of the particles on the mirror. The image processing analysis in MATLAB has been developed and tailored for the mirror images. Further improvements to the MATLAB code have been successfully realised. The computational time has been reduced by fine-tuning the two main parameters in the algorithm of image reconstruction by making a trade-off between a good quality of the reconstructed image and the computational time. For speeding up the process of dust deposition on the mirror surface, we have introduced in the experimental set-up an artificial dust deposition system. We deposit monodispersed silica spheres of diameter $\simeq$ 16 µm diluted in ultraclean propanol with a controlled spray system, and at each spray (or run) we register the interferometric signal and in the meantime, we register a picture of the mirror both before and after each spray. We then apply the image processing analysis on the consecutive images to detect the apparition of particles. The results of the first simultaneous measurements of the CBS signal and image processing on the pictures of the mirror under test are presented in this article. From the comparison of the experimental data with Mie theory, we can see that the basckscattering signal expected from theory for the particles having diameter (16 ± 6) µm is lower than the measured one. This can be attributed to the fact that on the mirror under test foreign, uncontrolled dust particles contribute to the CBS signal and prevent from observing the expected dependence of the backscattering amplitude with the number of particles. Efforts to improve the cleanliness and to reduce the quantity of unintended dust contamination should improve the agreement.

This should be feasible since the excess of CBS is known and is of the same order of magnitude of the expected signal. The presented results show that our table-top experiment is an important test bench for the study of the backscattered light issue for LISA interferometric measurements, nevertheless, more data sets need to be collected and analysed. We foresee to upgrade the present experimental set-up and realise measurements while scanning all the mirror surface, measurements with spontaneous dust deposition on the mirror under test, and measurements in conditions closer to those of LISA: heterodyne instead of homodyne, IR laser of wavelength 1.064 μm instead of 1.542 μm.

Acknowledgement: This work is co-funded by: Region PACA, Thales Alenia Space, Observatoire de la Cote d'Azur, CNES and CNRS.
We also acknowledge the interesting discussions on photography with E. Bonfanti.

References

[1] LISA-ESA webpage, http://sci.esa.int/lisa/
[2] Danzmann, K., Amaro-Seoane, P., Audley, H., Babak, S., Baker, J., Barausse, E., Bender, P., et al. (LISA Scientific Consortium), LISA proposal in response to the ESA call for L3 mission concept, 2017, Sec. 5.2.4, https://www.elisascience.org/files/publications/LISA_L3_20170120.pdf
[3] Naticchioni, L., Perciballi, M., Ricci, F., Coccia, E., Malvezzi, V., Acerneseet, F., et al., Microseismic Studies of an Underground Site for a New Interferometric Gravitational Wave Detector, Class. Quantum Grav. 31, 2014, 105016
[4] Dabbech, A., Deconvolution of Images in Centimeter-Band Radio Astronomy for the Exploitation of New Radio Interferometers: Characterization of Non Thermal Components in Galaxy Clusters, PhD Thesis, 2015, University of Nice Sophia Antipolis, Nice, France
[5] Born, M. & Wolf, E., Principles of Optics, 4th Ed., Pergamon Press Ltd., Oxford, 1970.
[6] Bohren, C.F. & Huffman, D.R., Absorption and Scattering of Light by Small Particles, John Wiley & Sons Inc., US, 1983.
[7] Abramowitz, M. & Stegun, I.A. Handbook of Mathematical Functions, Department of Commerce, National Bureau of Standards, Applied Mathematics Series 55, US, 1964, pp. 360